v. 4, n. 9, 2024

Journal of
Engineering
Research

ORBITS OF ARTIFICIAL MOON SATELLITES CONSIDERING THEIR NON-UNIFORM MASS DISTRIBUTION

Melissa Frigi Mendes

Rodolpho Vilhena de Moraes

Abstract: Artificial satellites are used in various activities, among which we can mention: space exploration, carrying out experiments in a micro gravity environment, geodynamic studies, climate monitoring, etc. This way, artificial satellites have made it possible to move the horizon of observations to distances unattainable from our planet, but for measurements made through satellites to be conveniently used, it is essential that their orbits and altitudes are known, at each instant, with precision. suitable for the purposes of the mission for which the satellite was planned. Hence the need to construct special theories or methods, generally adapted to specific missions. Based on this premise, in this present work, using Lagrange's planetary equations, variations in orbital elements of lunar satellites due to the non-uniform mass distribution of the Moon are analyzed, considering some coefficients associated with harmonics of lower order and degree than 9, for some initial conditions. Approximate analytical solutions are compared with the numerical integration of equations for some astrodynamics simulations, among which are carried out through programs created in Python language, to calculate variations in orbital elements, considering simplified models for the perturbations.
Keywords: Artificial satellites. Astrodynamics. Lunar satellites.

INTRODUCTION

Artificial satellites have made it possible to move the horizon of observations to distances unattainable from our planet and are used in various activities, including: space exploration, carrying out experiments in a micro-gravity environment, geodynamic studies, climate monitoring, study of the atmosphere and the earth's magnetic field, as a link in telecommunications, military applications, etc.

Artificial lunar satellites began to be placed into orbit initially in the 1960s during the Cold War period and the Space Race, more precisely by the Soviet Union on March 31, 1966 within a series of lunar missions called Luna, when it launched the first satellite artificial lunar called Luna 10. Following the success of the mission, several others were carried out in succession, such as the missions called Change carried out by China, and are still ongoing with the Change 5 mission. There are more countries that carry out lunar missions, and many of them involve satellites destined to orbit the moon for various research reasons, and this arouses interest and curiosity in many academic areas generating new areas of related research.

Within such a context, so that measurements made using satellites can be conveniently used, it is essential that their orbits and attitudes are known, at all times, with precision appropriate to the purposes of the mission for which the satellite was planned. Hence the need to construct special theories or methods, generally adapted to specific missions.

When studying the potential of an artificial satellite around the Moon using Legendre polynomials, it is observed that the order of magnitude of some coefficients associated with the order and degree of the polynomials are not hierarchically proportional to the order and degree of the polynomials. For example, unlike the case of Earth, the order of the coefficient associated with C22 is only one tenth smaller than the coefficient associated with J2; also, as an example, the order of magnitude of the coefficient associated with J9 is greater than the order of magnitude of the coefficient associated with J3. This makes the behavior of the orbital movement of lunar satellites, in some aspects, different from the behavior of the orbital movement of artificial Earth satellites.

OBJECTIVE

This project aims, using Lagrange's planetary equations and concepts of celestial mechanics, to analyze the variations in orbital elements of lunar satellites due to the non-uniform mass distribution of the Moon, considering some coefficients associated with harmonics of lower order and degree than 9, for some initial conditions. Approximate analytical solutions are compared with the numerical integration of the equations for some simulations carried out entirely in the Python language.

DEVELOPMENT

The initial concepts for understanding and carrying out this work begin with the 2-body problem, a theory of general mechanics related to Keplerian movements.

BODY PROBLEM

Given an inertial system with origin coordinates 0, we have 2 material points with masses m_1 and m_2, respectively, located at points P_1 and P_2. According to Newton's Law, such bodies attract each other according to the equation:

$$\overrightarrow{f_{1,2}} = -\mathrm{G}m_1m_2\,\frac{P_1-P_2}{r^3} \tag{2.1}$$

Where G is the universal gravitational constant and r, modulus of $\vec{r}$, is the distance from P_i.e. P_j. We want to determine the movement of P_1 and P_2 and for this we have the following equations:

$$m_1\ddot{\vec{r}}_1 = -\frac{Gm_1m_2}{r^2}\,\frac{P_1-P_2}{r} \tag{2.2}$$

$$m_2\ddot{\vec{r}}_2 = -\frac{Gm_1m_2}{r^2}\,\frac{P_2-P_1}{r} \tag{2.3}$$

From these, a system of 6 second-order differential equations, or 12 first-order differential equations, is formed, which requires 12 integration constants for its complete solution.

We have the vector equation that describes such movement of P_1 in relation to P_2 is given by:

$$\ddot{\vec{r}} = -\frac{\mu}{r^2}\frac{\vec{r}}{r} \tag{2.4}$$

Being:

$$\mu = G\,(m_1 + m_1) \tag{2.5}$$

These equations form a system of order 6 that, to solve it, it is necessary to use the integrals of the center of mass, to arrive at the final radius equation:

$$r = \frac{P}{1+e\cos(\varphi-\omega)} \tag{2.6}$$

Being:

$$P = \frac{C^2}{\mu} = a(1-e^2) \tag{2.7}$$

Like this,

$$e = \sqrt{\frac{2EC}{\mu^2} - 1} \tag{2.8}$$

Note that r is an equation of a conic in polar coordinates with P being the semi latusrectum, a is the semi major axis, e is the eccentricity of the conic, $(\varphi - \omega)$ is the angle polar, and E and C are constants where $C = r^2\varphi$ e $E = \frac{1}{2}\dot{\vec{r}}^{\,2} - \frac{\mu}{r}$.

Therefore, if $E < 0$ and $e < 1$, the conic will be an ellipse and is the premise for the parameters worked on in this project.

KEPLERIAN ORBITAL ELEMENTS

In celestial mechanics there is a set of 6 parameters that describe an orbital movement, also called Keplerian orbital elements, of which we can mention in the elliptical case: the semi-major axis of the orbit (a), that is, the distance from the center of the ellipse to the perihelion; eccentricity of the orbit

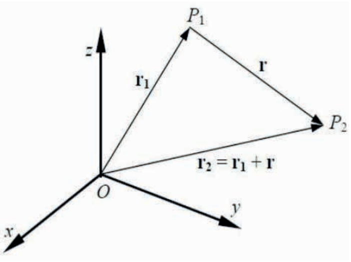

Figure 2.1 - Coordinate system in the 2-body problem.

Source: Kuga et al., 2008.

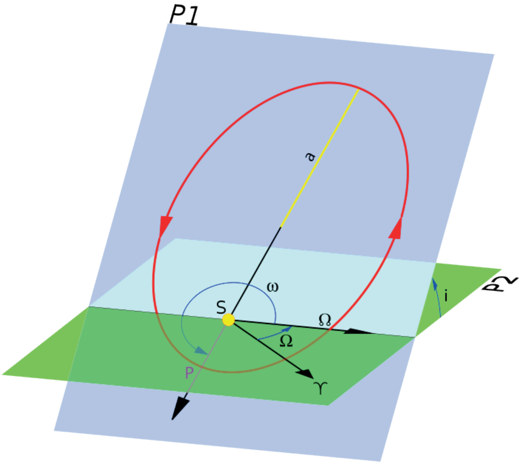

Figure 2.2 – Orbital elements of a celestial body.

Source: Wikipedia, Orbital Elements.

Figure 2.3 - Sector Harmonics.

Source: Kuga et al., 2011.

Figure 2.4 - Zonal Harmonics.

Source: Kuga et al., 2011.

Figure 2.5 - Tesseral Harmonics.

Source: Kuga et al., 2011.

Coefficients	
J_2	$+2.070 \times 10^{-4}$
J_3	$+4.900 \times 10^{-6}$
J_4	$+8.000 \times 10^{-7}$
J_5	-3.600×10^{-6}
J_6	-1.100×10^{-6}
J_7	-2.870×10^{-5}
C_{22}	$+2.447305 \times 10^{-5}$

Figure 2.4 - Zonal and Sectoral Harmonics

Source: Carvalho et al. (2011)

(e), which represents the ratio between half the distance between the foci and the semi-major axis; orbital inclination (i) measures the angle between the reference plane and the orbital plane; the pericenter argument (ω) is the angle measured in the body's orbital plane between the ascending node and the pericenter, corresponding to its direction of rotation; the right ascension of the ascending node (Ω), or ascending node longitude, is the ecliptic longitude of the ascending node of the orbit; and, finally, the average anomaly (M) is the conversion to angle at the time of the body's passage through periastron.

We also have that 'a', 'e' and 'i' are called metric variables, and 'ω', 'Ω' and 'M' as the angular variables.

GRAVITATIONAL POTENTIAL

Be it an artificial satellite under the gravitational potential force of a central body, and orbiting a body with non-uniform distribution of mass, the following expression for the gravitational potential is considered (Morando, 1974):

$$U = \frac{\mu}{r}\left[1 - \sum_{n=2}^{\infty} \frac{J_n a_e^n}{r^n} P_n(sen\phi) + \sum_{n=2}^{\infty}\sum_{m=1}^{n} \frac{J_{n,m} a_e^n}{r^n} P_{n,m}(sen\phi)\cos m(\lambda - \lambda_{n,m})\right] \tag{2.9}$$

Where μ is the gravitational constant, r represents the distance between the satellite and the center of mass of the body with non-uniform distribution of mass, Jn, Jn, m and λn, m are elements of the central body, ae is the equatorial radius of the body central, the indices nor represent the degree and order of the associated Legendre polynomial, Pn, m are the associated Legendre polynomials, and the angles ϕ and λ represent latitude and longitude in angles.

Below are three examples of harmonics in spherical bodies: sectoral, zonal and tesseral. Zonal harmonics are polynomials of degree n, being m = 0 and independent of the longitude λ, the zonal harmonics divide the sphere into positive and negative sectors and have degrees n = m, and the tesseral harmonics have cosmλ functions and degree 2m.

In this project, the following zonal coefficients of J are used2 to J_6 for the moon, also highlighting the importance of the elements J_7, which is still under development, and the sectoral harmonic C_{22}.

LAGRANGE PLANETARY EQUATIONS

Lagrange's planetary equations allow you to determine the speed and location of a celestial body in an orbit, and are described in terms of the previously mentioned Keplerian orbital elements:

$$\frac{da}{dt} = \frac{2}{na}\frac{\partial R}{\partial M} \tag{2.10}$$

$$\frac{de}{dt} = \frac{-\sqrt{1-e^2}}{na^2 e}\frac{\partial R}{\partial \omega} + \frac{1-e^2}{na^2 e}\frac{\partial R}{\partial M} \tag{2.11}$$

$$\frac{di}{dt} = \frac{-1}{na^2\sqrt{1-e^2}\,sen\,i}\frac{\partial R}{\partial \Omega} + \frac{cos\,i}{na^2\sqrt{1-e^2}\,sen\,i}\frac{\partial R}{\partial \omega} \tag{2.12}$$

$$\frac{d\Omega}{dt} = \frac{1}{na^2\sqrt{1-e^2}\,sen\,i}\frac{\partial R}{\partial i} \tag{2.13}$$

$$\frac{d\omega}{dt} = \frac{\sqrt{1-e^2}}{na^2 e}\frac{\partial R}{\partial e} - \frac{cos\,i}{na^2\sqrt{1-e^2}\,sen\,i}\frac{\partial R}{\partial i} \tag{2.14}$$

$$\frac{dM}{dt} = n - \frac{2}{na}\frac{\partial R}{\partial a} - \frac{1-e^2}{na^2 e}\frac{\partial R}{\partial e} \tag{2.15}$$

The expressions that contain $\frac{\partial R}{\partial M}$ and $\frac{\partial R}{\partial \Omega}$, in this case, are called short equations period, and those containing $\frac{\partial R}{\partial \omega}$, $\frac{\partial R}{\partial i}$, $\frac{\partial R}{\partial e}$ and $\frac{\partial R}{\partial a}$, are called long period. The proposal this project involves only long-period equations, but the importance of short-period equational elements is highlighted for a more elaborate study of disturbances.

Journal of Engineering Research ISSN 2764-1317 DOI: https://doi.org/10.22533/at.ed.317492414039

PERTURBATION FUNCTIONS

Below are the disturbance functions as a function of the zonal harmonics J2 to J6 and the C22 harmonic of the moon used throughout this research, obtained from the scientific article Planetary Satellite Orbiters: Applications for the Moon (Carvalho et al., 2011):

$$\langle\langle R_{J_2}\rangle\rangle = -\frac{1}{4} R_M^2 J_2 \frac{n^2}{(1-e^2)^{3/2}}(-2+3s_i^2), \tag{2.16}$$

$$\langle\langle R_{J_3}\rangle\rangle = -\frac{3}{8} R_M^3 J_3 \frac{n^2 s_i e}{a(1-e^2)^{5/2}}(-4+5s_i^2)\sin\omega, \tag{2.17}$$

$$\langle\langle R_{J_4}\rangle\rangle = \frac{3}{128} R_M^4 J_4 \frac{n^2}{a^2(1-e^2)^{7/2}} \times \left(10e^2 s_i^2(7s_i^2-6)\cos(2\omega) - (3e^2+2)(35s_i^4-40s_i^2+8)\right), \tag{2.18}$$

$$\begin{aligned}\langle\langle R_{J_5}\rangle\rangle = \frac{5}{256} R_M^5 J_5 \frac{n^2 s_i e}{a^3(1-e^2)^{9/2}} &\times (14e^2 s_i^2(9s_i^2-8)\cos(2\omega) + e^2(-315s_i^4+448s_i^2-144) \\ &-24(21s_i^4-28s_i^2+8))\sin\omega,\end{aligned} \tag{2.19}$$

$$\begin{aligned}\langle\langle R_{J_6}\rangle\rangle = -\frac{5}{4096} R_M^6 J_6 \frac{n^2}{a^4(1-e^2)^{11/2}} &\times (-2(15e^4+40e^2+8)(231s_i^6-378s_i^4+168s_i^2-16) \\ &-63e^4(11s_i^2-10)s_i^4\cos(4\omega) + 210e^2(e^2+2) \\ &\times (33s_i^4-48s_i^2+16)s_i^2\cos(2\omega)),\end{aligned} \tag{2.20}$$

$$\langle\langle R_{C_{22}}\rangle\rangle = \frac{3}{2} R_M^2 \overline{C}_{22} \frac{n^2}{(1-e^2)^{3/2}} s_i^2 \cos(2(\Omega - \gamma_M t)) \tag{2.21}$$

It is necessary to mention that the equation for RJ_7 is in the development process by the author and, as RC_{22} contains short period terms, it was not used in the development process in this study.

ANGULAR ELEMENT VARIATIONS

The expressions for the variation of angular elements used as parameters in the development of the graphics shown during the following topics were published by B. Morando (1974):

$$\omega = n_\omega t + \omega_0 = \left(nJ_2\left(\frac{a_e}{a}\right)^2 \frac{1}{(1-e^2)^2}\left(-\frac{3}{5}+\frac{15}{4}\cos^2 i\right)\right)t + \omega_0 \tag{2.22}$$

$$\Omega = n_\Omega t + \Omega_0 = \left(-nJ_2\left(\frac{a_e}{a}\right)^2 \frac{1}{(1-e^2)^2}\frac{3}{2}\cos i\right)t + \Omega_0 \tag{2.23}$$

$$M = nt + n_M t + M_0 = nt + \left(3nJ_2\left(\frac{a_e}{a}\right)^2 \left(-\frac{1}{4}+\frac{3}{4}\cos^2 i\right)\left(1-e^2\right)^{-\frac{3}{2}}\right)t + M_0 \tag{2.24}$$

Where n represents the average movement in degrees per day of the celestial body, with $n = \sqrt{\mu \cdot a^3}$, Ω_0 is the initial value of the longitude at the ascending node, ω_0 is the initial value of the pericenter argument and M_0 is the initial value of the mean anomaly. All values of the constants used in the calculations of such equations, as well as the results obtained, are contained in Parameters 1 and 2 shown in the following topic.

SIMULATIONS AND RESULTS

Firstly, with the equations of the previously mentioned perturbation functions, a program in Python language was created to calculate the partial derivatives of each of them considering each zonal harmonic J_1 to J_6. Note that in RJ_2 there is no constant ω and a, so the derivatives of $\partial RJ_2/\partial\omega$ and $\partial RJ_2/\partial a$ will result in 0.

∂R/∂i result for RJ2:

$$-\frac{1.5 J dois RaioL^2 i n^2}{(1-e^2)^{1.5}} \tag{2.25}$$

∂R/∂e result for RJ2:

$$-\frac{0.75 J dois RaioL^2 e n^2 \cdot (3i^2-2)}{(1-e^2)^{2.5}} \tag{2.26}$$

∂R/∂ω result for RJ3:

$$-\frac{0.375 J tres RaioL^3 e i n^2 \cdot (5i^2-4)\cos(w)}{a(1-e^2)^{2.5}} \tag{2.27}$$

∂R/∂a result for RJ3:

$$\frac{0.375 J tres RaioL^3 e i n^2 \cdot (5i^2-4)\sin(w)}{a^2(1-e^2)^{2.5}} \tag{2.28}$$

∂R/∂i result for RJ3:

$$-\frac{3.75 JtresRaioL^{3} e i^{2} n^{2}\sin(w)}{a\left(1-e^{2}\right)^{2.5}}-\frac{0.375 JtresRaioL^{3} e n^{2}\cdot\left(5i^{2}-4\right)\sin(w)}{a\left(1-e^{2}\right)^{2.5}} \tag{2.29}$$

∂R/∂e result for RJ3:

$$-\frac{1.875 JtresRaioL^{3} e^{2} i n^{2}\cdot\left(5i^{2}-4\right)\sin(w)}{a\left(1-e^{2}\right)^{3.5}}-\frac{0.375 JtresRaioL^{3} i n^{2}\cdot\left(5i^{2}-4\right)\sin(w)}{a\left(1-e^{2}\right)^{2.5}} \tag{2.30}$$

∂R/∂ω result for RJ4:

$$-\frac{0.46875 JquatroRaioL^{4} e^{2} i^{2} n^{2}\cdot\left(7i^{2}-6\right)\sin(2w)}{a\left(1-e^{2}\right)^{3.5}} \tag{2.31}$$

∂R/∂a result for RJ4:

$$-\frac{0.0234375 JquatroRaioL^{4} n^{2}\cdot\left(10e^{2}i^{2}\cdot\left(7i^{2}-6\right)\cos(2w)-\left(3e^{2}+2\right)\left(35i^{4}-40i^{2}+8\right)\right)}{a^{2}\left(1-e^{2}\right)^{3.5}} \tag{2.32}$$

∂R/∂i result for RJ4:

$$\frac{0.0234375 JquatroRaioL^{4} n^{2}\cdot\left(140e^{2}i^{3}\cos(2w)+20e^{2}i\left(7i^{2}-6\right)\cos(2w)+\left(-3e^{2}-2\right)\left(140i^{3}-80i\right)\right)}{a\left(1-e^{2}\right)^{3.5}} \tag{2.33}$$

∂R/∂e result for RJ4:

$$\frac{0.1640625 JquatroRaioL^{4} e n^{2}\cdot\left(10e^{2}i^{2}\cdot\left(7i^{2}-6\right)\cos(2w)-\left(3e^{2}+2\right)\left(35i^{4}-40i^{2}+8\right)\right)}{a\left(1-e^{2}\right)^{4.5}}+\frac{0.0234375 JquatroRaioL^{4} n^{2}\cdot\left(20 e i^{2}\cdot\left(7i^{2}-6\right)\cos(2w)-6e\left(35i^{4}-40i^{2}+8\right)\right)}{a\left(1-e^{2}\right)^{3.5}} \tag{2.34}$$

∂R/∂ω result for RJ5:

$$-\frac{0.546875 J_{5} RaioL^{5} e^{3} i^{3} n^{2}\cdot\left(9i^{2}-8\right)\sin(w)\sin(2w)}{a^{3}\left(1-e^{2}\right)^{4.5}}+\frac{0.01953125 J_{5} RaioL^{5} e i n^{2}\cdot\left(14e^{2}i^{2}\cdot\left(9i^{2}-8\right)\cos(2w)+e^{2}\left(-315i^{4}+448i^{2}-144\right)-504i^{4}+672i^{2}-192\right)\cos(w)}{a^{3}\left(1-e^{2}\right)^{4.5}} \tag{2.35}$$

∂R/∂a result for RJ5:

$$-\frac{0.05859375 J_{5} RaioL^{5} e i n^{2}\cdot\left(14e^{2}i^{2}\cdot\left(9i^{2}-8\right)\cos(2w)+e^{2}\left(-315i^{4}+448i^{2}-144\right)-504i^{4}+672i^{2}-192\right)\sin(w)}{a^{4}\left(1-e^{2}\right)^{4.5}} \tag{2.36}$$

∂R/∂i result for RJ5:

$$\frac{0.01953125 J_{5} RaioL^{5} e i n^{2}\cdot\left(252e^{2}i^{3}\cos(2w)+28e^{2}i\left(9i^{2}-8\right)\cos(2w)+e^{2}\left(-1260i^{3}+896i\right)-2016i^{3}+1344i\right)\sin(w)}{a^{3}\left(1-e^{2}\right)^{4.5}}+\frac{0.01953125 J_{5} RaioL^{5} e n^{2}\cdot\left(14e^{2}i^{2}\cdot\left(9i^{2}-8\right)\cos(2w)+e^{2}\left(-315i^{4}+448i^{2}-144\right)-504i^{4}+672i^{2}-192\right)\sin(w)}{a^{3}\left(1-e^{2}\right)^{4.5}} \tag{2.37}$$

Journal of Engineering Research ISSN 2764-1317 DOI: https://doi.org/10.22533/at.ed.317492414039

∂R/∂e result for RJ5:

$$\frac{0.17578125 J_5 RaioL^5 e^2 i n^2 \cdot \left(14e^2 i^2 \cdot \left(9i^2-8\right)\cos(2w) + e^2\left(-315i^4+448i^2-144\right) - 504i^4 + 672i^2 - 192\right)\sin(w)}{a^3\left(1-e^2\right)^{5.5}} + \frac{0.01953125 J_5 RaioL^5 e i n^2 \cdot \left(28ei^2 \cdot \left(9i^2-8\right)\cos(2w) + 2e\left(-315i^4+448i^2-144\right)\right)\sin(w)}{a^3\left(1-e^2\right)^{4.5}} + \frac{0.01953125 J_5 RaioL^5 i n^2 \cdot \left(14e^2 i^2 \cdot \left(9i^2-8\right)\cos(2w) + e^2\left(-315i^4+448i^2-144\right) - 504i^4 + 672i^2 - 192\right)\sin(w)}{a^3\left(1-e^2\right)^{4.5}} \tag{2.38}$$

∂R/∂ω result for RJ6:

$$-\frac{0.001220703125 J_6 RaioL^6 n^2 \cdot \left(252e^4 i^4 \cdot \left(11i^2-10\right)\sin(4w) - 420e^2 i^2\left(e^2+2\right)\left(33i^4-48i^2+16\right)\sin(2w)\right)}{a^4\left(1-e^2\right)^{5.5}} \tag{2.39}$$

∂R/∂a result for RJ6:

$$\frac{0.0048828125 J_6 RaioL^6 n^2\left(-63e^4 i^4 \cdot \left(11i^2-10\right)\cos(4w) + 210e^2 i^2\left(e^2+2\right)\left(33i^4-48i^2+16\right)\cos(2w) + \left(-30e^4-80e^2-16\right)\left(231i^6-378i^4+168i^2-16\right)\right)}{a^5\left(1-e^2\right)^{5.5}} \tag{2.40}$$

∂R/∂i result for RJ6:

$$-\frac{0.001220703125 J_6 RaioL^6 n^2\left(-1386e^4 i^5\cos(4w) - 252e^4 i^3 \cdot \left(11i^2-10\right)\cos(4w) + 210e^2 i^2\left(e^2+2\right)\left(132i^3-96i\right)\cos(2w) + 420e^2 i\left(e^2+2\right)\left(33i^4-48i^2+16\right)\cos(2w) + \left(-30e^4-80e^2-16\right)\left(1386i^5-1512i^3+336i\right)\right)}{a^4\left(1-e^2\right)^{5.5}} \tag{2.41}$$

∂R/∂e result for RJ6:

$$-\frac{0.013427734375 J_6 RaioL^6 e n^2\left(-63e^4 i^4 \cdot \left(11i^2-10\right)\cos(4w) + 210e^2 i^2\left(e^2+2\right)\left(33i^4-48i^2+16\right)\cos(2w) + \left(-30e^4-80e^2-16\right)\left(231i^6-378i^4+168i^2-16\right)\right)}{a^4\left(1-e^2\right)^{6.5}} - \frac{0.001220703125 J_6 RaioL^6 n^2\left(-252e^3 i^4 \cdot \left(11i^2-10\right)\cos(4w) + 420e^3 i^2 \cdot \left(33i^4-48i^2+16\right)\cos(2w) + 420ei^2\left(e^2+2\right)\left(33i^4-48i^2+16\right)\cos(2w) + \left(-120e^3-160e\right)\left(231i^6-378i^4+168i^2-16\right)\right)}{a^4\left(1-e^2\right)^{5.5}} \tag{2.42}$$

After calculating the partial derivatives of the disturbance functions, it was possible to complete the Lagrange equations (2.16) to (2.21) for each harmonic Jn as shown below:

Lagrange equation dΩ/dt for J2:

$$-\frac{1.5 JdoisRaioL^2 in}{a^2\left(1-e^2\right)^{2.0}\sin(i)} \tag{2.43}$$

Lagrange equation from/dt to J2: 0.

Lagrange equation dω/dt for J2:

$$\frac{1.5 JdoisRaioL^2 in\cos(i)}{a^2\left(1-e^2\right)^{2.0}\sin(i)} - \frac{0.75 JdoisRaioL^2 n\left(3i^2-2\right)}{a^2\left(1-e^2\right)^{2.0}} \tag{2.44}$$

Lagrange equation dM/dt for J2:

$$\frac{0.75 JdoisRaioL^2 n\left(3i^2-2\right)}{a^2\left(1-e^2\right)^{1.5}} + n \tag{2.45}$$

Lagrange equation di/dt for J2: 0

Lagrange equation dΩ/dt for J3:

$$\frac{-\frac{3.75 JtresRaioL^{3} e i^{2} n^{2} \sin(w)}{a(1-e^{2})^{2.5}} - \frac{0.375 JtresRaioL^{3} e n^{2} \cdot (5i^{2}-4) \sin(w)}{a(1-e^{2})^{2.5}}}{a^{2} n \sqrt{1-e^{2}} \sin(i)} \tag{2.46}$$

Lagrange equation from/dt to J3:

$$\frac{0.375 JtresRaioL^{3} i n \left(5i^{2}-4\right) \cos(w)}{a^{3}\left(1-e^{2}\right)^{2.0}} \tag{2.47}$$

Lagrange equation dM/dt for J3:

$$-\frac{0.75 JtresRaioL^{3} e i n \left(5i^{2}-4\right) \sin(w)}{a\left(1-e^{2}\right)^{2.5}} + n - \frac{\left(1-e^{2}\right)\left(-\frac{1.875 JtresRaioL^{3} e^{2} i n^{2} \cdot (5i^{2}-4) \sin(w)}{a(1-e^{2})^{3.5}} - \frac{0.375 JtresRaioL^{3} i n^{2} \cdot (5i^{2}-4) \sin(w)}{a(1-e^{2})^{2.5}}\right)}{a^{2} e n} \tag{2.48}$$

Lagrange equation dω/dt for J3:

$$-\frac{\left(-\frac{3.75 JtresRaioL^{3} e i^{2} n^{2} \sin(w)}{a(1-e^{2})^{2.5}} - \frac{0.375 JtresRaioL^{3} e n^{2} \cdot (5i^{2}-4) \sin(w)}{a(1-e^{2})^{2.5}}\right) \cos(i)}{a^{2} n \sqrt{1-e^{2}} \sin(i)} + \frac{\sqrt{1-e^{2}} \left(-\frac{1.875 JtresRaioL^{3} e^{2} i n^{2} \cdot (5i^{2}-4) \sin(w)}{a(1-e^{2})^{3.5}} - \frac{0.375 JtresRaioL^{3} i n^{2} \cdot (5i^{2}-4) \sin(w)}{a(1-e^{2})^{2.5}}\right)}{a^{2} e n} \tag{2.49}$$

Lagrange equation di/dt for J3:

$$-\frac{0.375 JtresRaioL^{3} e i n \left(5i^{2}-4\right) \cos(i) \cos(w)}{a^{3}\left(1-e^{2}\right)^{3.0} \sin(i)} \tag{2.50}$$

Lagrange equation dΩ/dt for J4:

$$\frac{0.0234375 JquatroRaioL^{4} n \left(140 e^{2} i^{3} \cos(2w) + 20 e^{2} i \left(7i^{2}-6\right) \cos(2w) + \left(-3e^{2}-2\right)\left(140 i^{3} - 80 i\right)\right)}{a^{3}\left(1-e^{2}\right)^{4.0} \sin(i)} \tag{2.51}$$

Lagrange equation from/dt to J4:

$$\frac{0.46875 JquatroRaioL^{4} e i^{2} n \left(7i^{2}-6\right) \sin(2w)}{a^{3}\left(1-e^{2}\right)^{3.0}} \tag{2.52}$$

Lagrange equation dω/dt for J4:

$$-\frac{0.0234375 JquatroRaioL^{4} n \left(140 e^{2} i^{3} \cos(2w) + 20 e^{2} i \left(7i^{2}-6\right) \cos(2w) + \left(-3e^{2}-2\right)\left(140 i^{3} - 80 i\right)\right) \cos(i)}{a^{3}\left(1-e^{2}\right)^{4.0} \sin(i)} + \frac{\sqrt{1-e^{2}} \cdot \left(\frac{0.1640625 JquatroRaioL^{4} e n^{2} \cdot \left(10 e^{2} i^{2} \cdot (7i^{2}-6) \cos(2w) - (3e^{2}+2)(35 i^{4} - 40 i^{2} + 8)\right)}{a(1-e^{2})^{4.5}} + \frac{0.0234375 JquatroRaioL^{4} n^{2} \cdot \left(20 e i^{2} \cdot (7i^{2}-6) \cos(2w) - 6e(35 i^{4} - 40 i^{2} + 8)\right)}{a(1-e^{2})^{3.5}}\right)}{a^{2} e n} \tag{2.53}$$

Lagrange equation dM/dt for J4:

$$n - \frac{2\left(-0.234375 JquatroRaioL^{4} e^{2} i^{2} n^{2} \cdot \left(7i^{2}-6\right) \cos(2w) - \left(3e^{2}+2\right)\left(35 i^{4} - 40 i^{2} + 8\right)\right)}{a n\left(1-e^{2}\right)^{3.5}} - \frac{\left(1-e^{2}\right)\left(\frac{0.1640625 JquatroRaioL^{4} e n^{2} \cdot \left(10 e^{2} i^{2} \cdot (7i^{2}-6) \cos(2w) - (3e^{2}+2)(35 i^{4} - 40 i^{2} + 8)\right)}{a(1-e^{2})^{4.5}} + \frac{0.0234375 JquatroRaioL^{4} n^{2} \cdot \left(20 e i^{2} \cdot (7i^{2}-6) \cos(2w) - 6e(35 i^{4} - 40 i^{2} + 8)\right)}{a(1-e^{2})^{3.5}}\right)}{a^{2} e n} \tag{2.54}$$

Lagrange equation di/dt for J4:

$$-\frac{0.46875 J\,quatroRaioL^4 e^2 i^2 n\left(7i^2-6\right)\sin\left(2w\right)\cos\left(i\right)}{a^3\left(1-e^2\right)^{4.0}\sin\left(i\right)} \quad (2.55)$$

The comparison graphs generated continue up to harmonic J4, so the Lagrange equations for J5 and J6 will not be necessary.

After calculating the period ne of the variations of the angular elements, 2 parameters were considered for the calculations of the integrals based on the Lagrange equations, parameter 1 considers the constant a1 = radius of the Moon + 50 km and a2 = radius of the Moon +100km, as well as the eccentricities e1 = 0.01 and e2 =0.02.

We have that parameters 1 are: n: 26.05130 rad/day = 1492.629541 degrees per day, Ω: -0.25286, ω: 0.60222, M: - 0.12313 and i: 30 degrees. Thus, the following graphs were obtained:

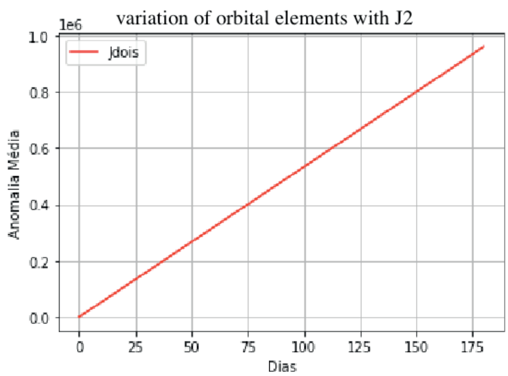

Figure 1 - Average Anomaly Graph with J2.

Source: Author's production.

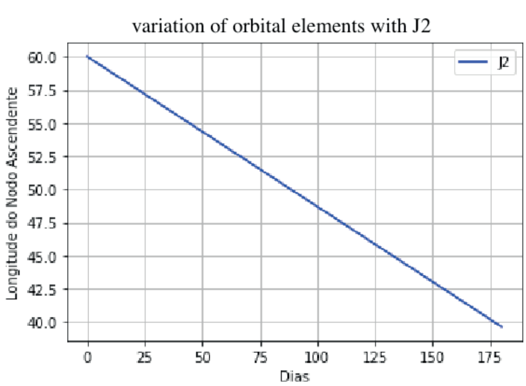

Figure 1 - Longitude Graph on the Ascending Node with J2.

Source: Author's production.

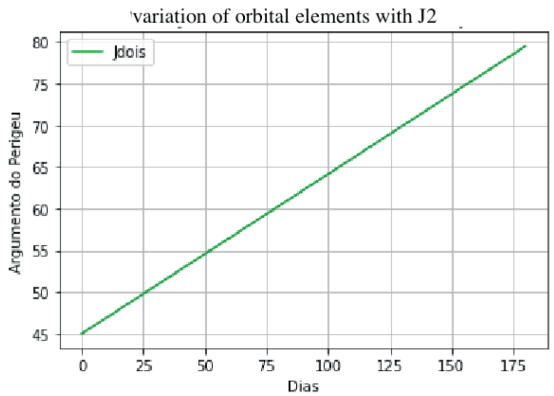

Figure 2 - Perigee Argument Graph with J2.

Source: Author's production.

For the J3 zonal harmonics, we obtained:

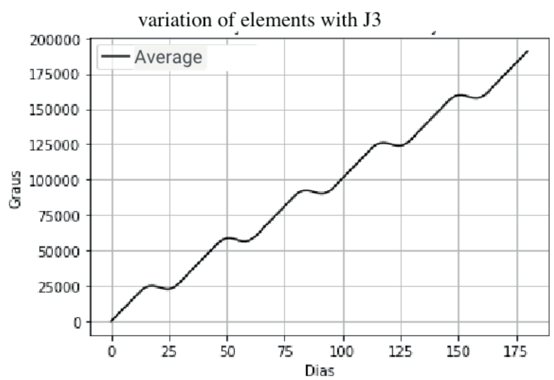

Figure 2.6 – Average Anomaly with J3.

Source: Author's production.

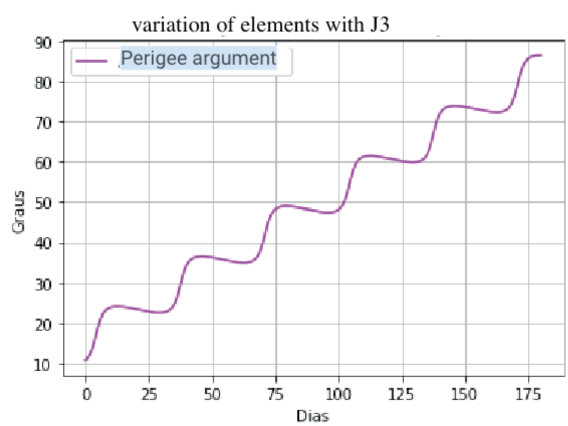

Figure 2.7 – Perigee Argument with J3.

Source: Author's production.

Journal of Engineering Research ISSN 2764-1317 DOI: https://doi.org/10.22533/at.ed.317492414039

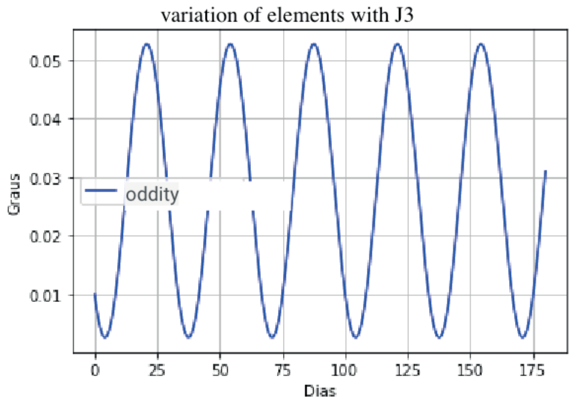

Figure 2.8 – Eccentricity with J3.

Source: Author's production.

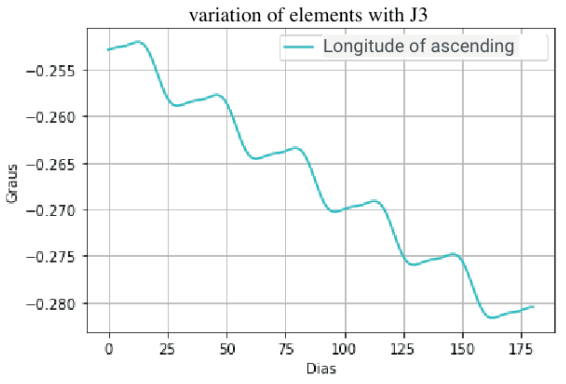

Figure 2.9 – Longitude of the Ascending Node with J3.

Source: Author's production.

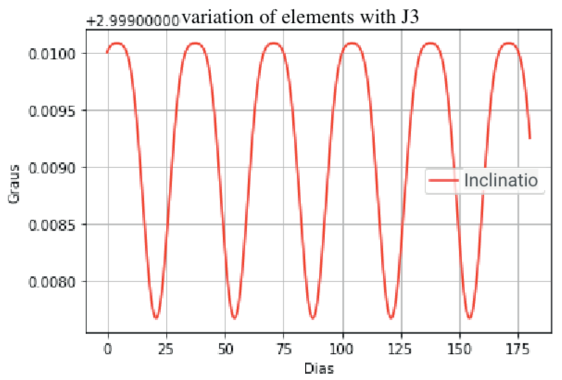

Figure 2.10 - Tilt with J3.

Source: Author's production.

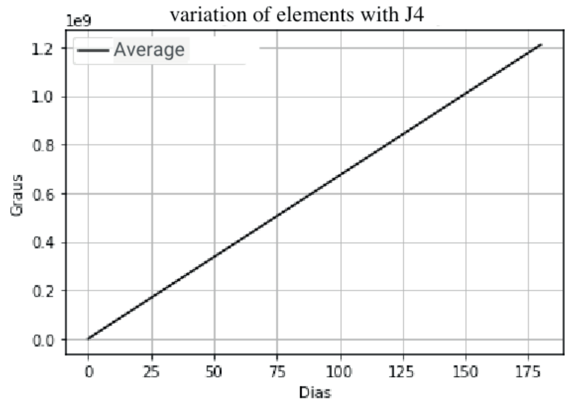

Figure 2.11 – Average Anomaly with J4.

Source: Author's production.

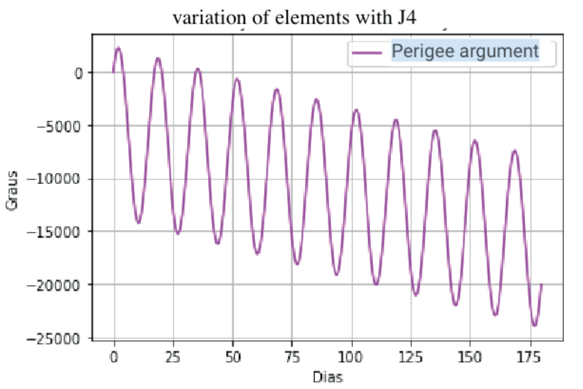

Figure 2.12 – Perigee Argument with J4.

Source: Author's production.

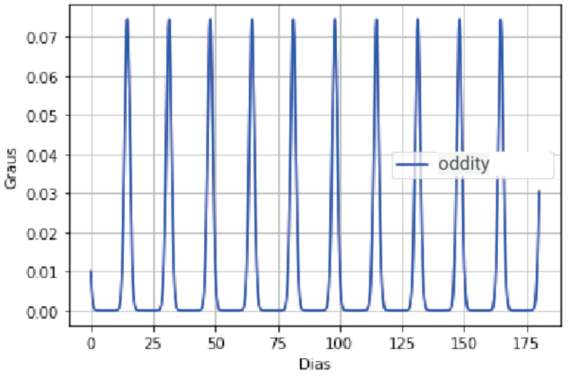

Figure 2.13 - Eccentricity with J4.

Source: Author's production.

For the J4 zonal harmonics, we have:

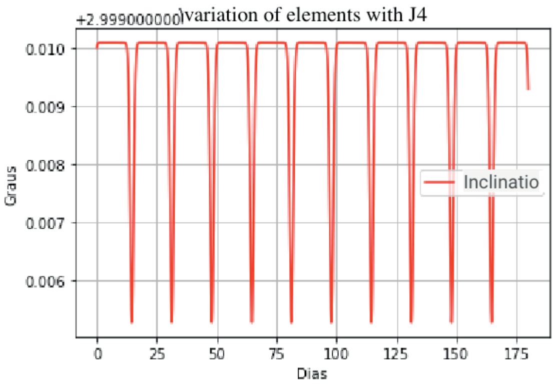

Figure 2.14 - Slope with J4.

Source: Author's production.

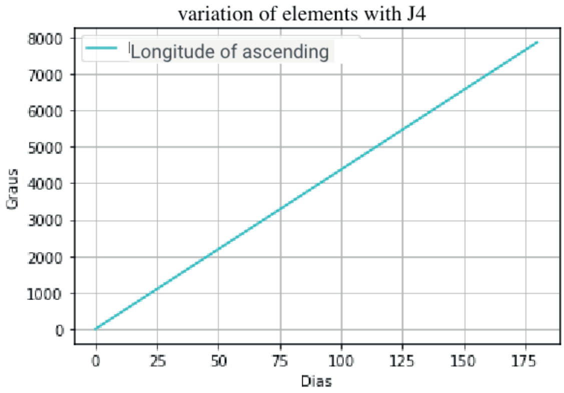

Figure 2.15 – Longitude of the Ascending Node with J4.

Source: Author's production.

Then it is known that the parameters 2 obtained are n: 25.69440 rad/day = 1472.180677 degrees per day, Ω: -0.23615, ω: 0.56242, M: -0.11488 and i: 30 degrees. This way, we obtain:

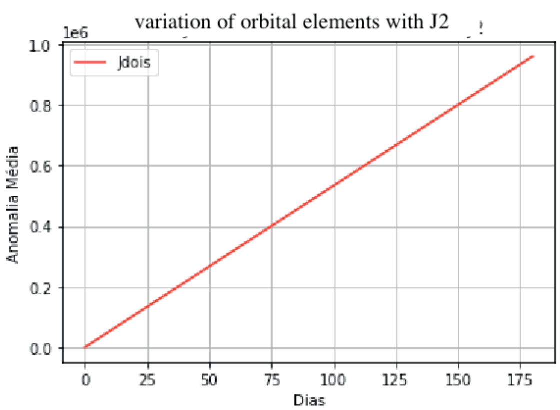

Figure 2.16 - Average Anomaly with J2 for parameters 2.

Source: Author's production.

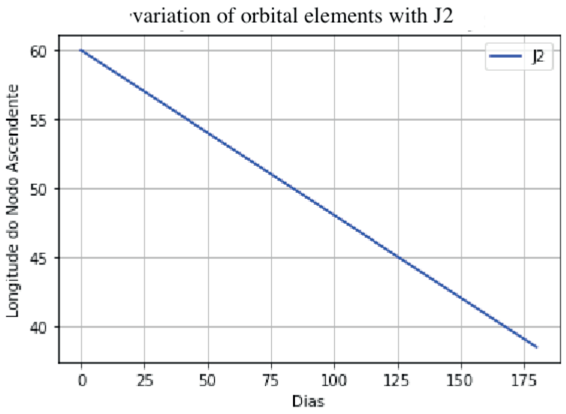

Figure 2.17 - Longitude of the Ascending Node with J2 for parameters 2.

Source: Author's production.

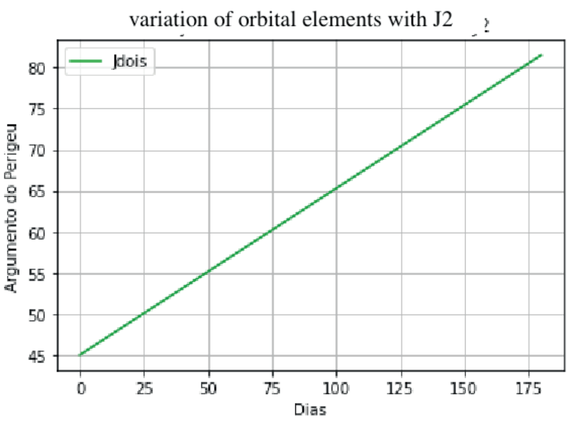

Figure 2.18 – Perigee argument with J2 for parameters 2.

Source: Author's production.

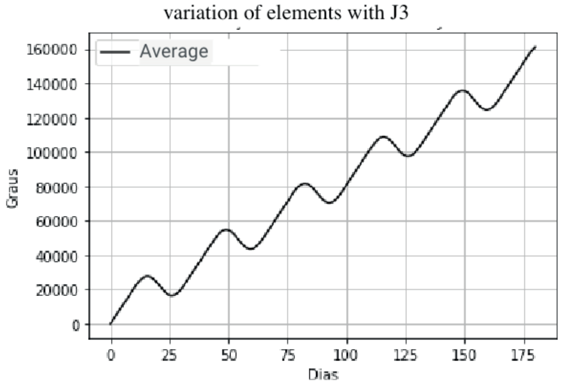

Figure 2.19 - Average Anomaly with J3 for parameters 2.

Source: Author's production.

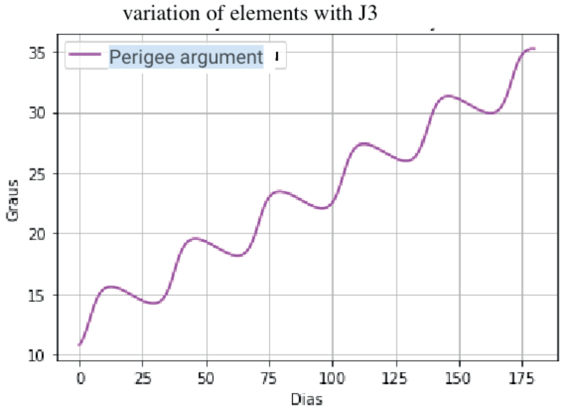

Figure 2.20 - Pericenter argument with J3 for parameters 2.

Source: Author's

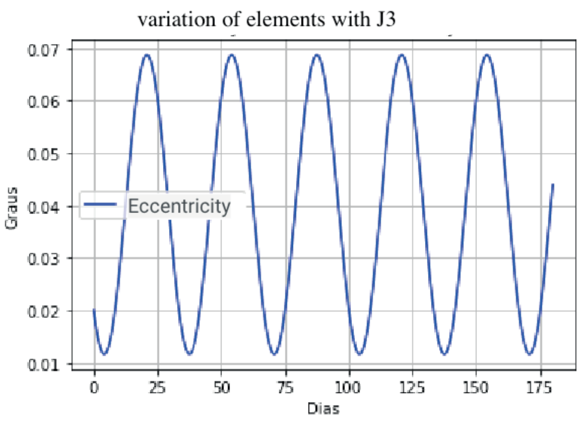

Figure 2.21 - Eccentricity with J3 for parameters 2.

Source: Author's production.

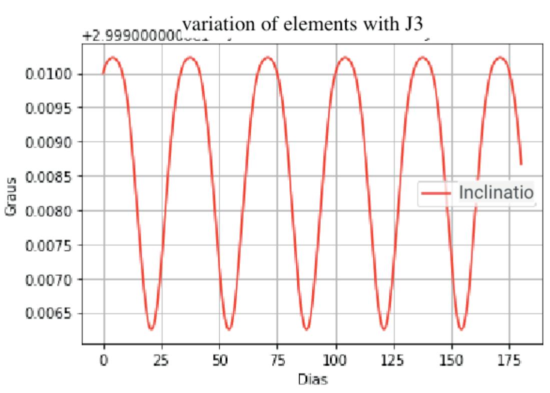

Figure 2.22 - Slope with J3 for parameters 2.

Source: Author's production.

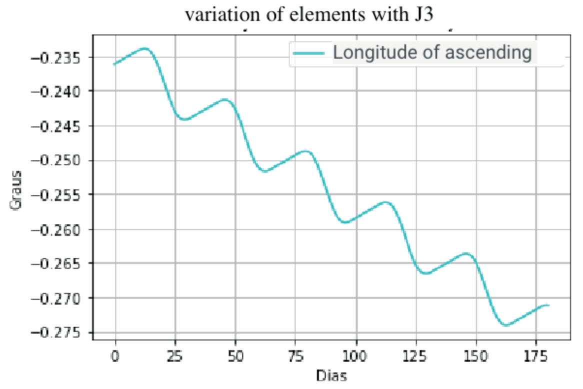

Figure 2.23 - Longitude at the Ascending Node with J3 for parameters 2.

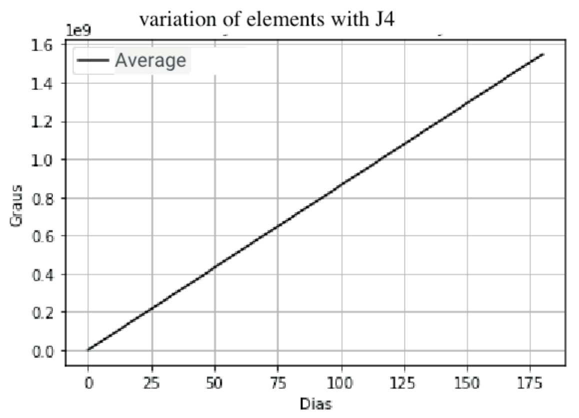

Figure 2.24 - Average Anomaly with J4 for parameters 2.

Source: Author's production.

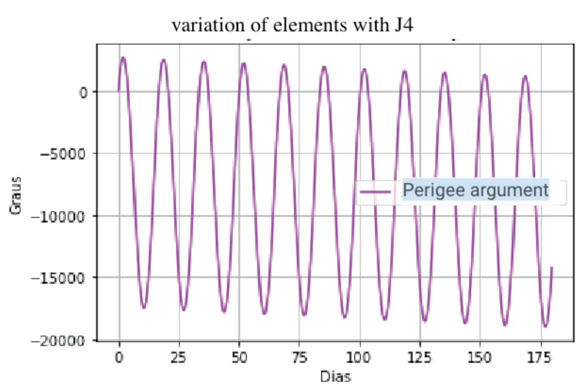

Figure 2.25 - Pericenter argument with J4 for parameters 2.

Source: Author's

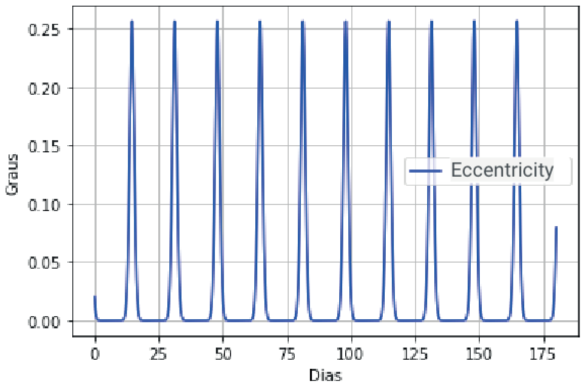

Figure 2.26 - Eccentricity with J4 for parameters 2.

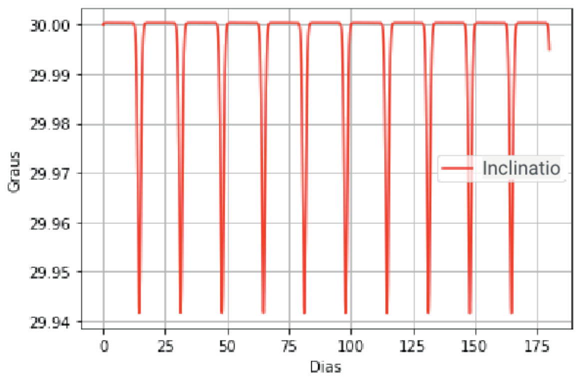

Figure 2.27 - Slope with J4 for parameters 2.

Source: Author's production.

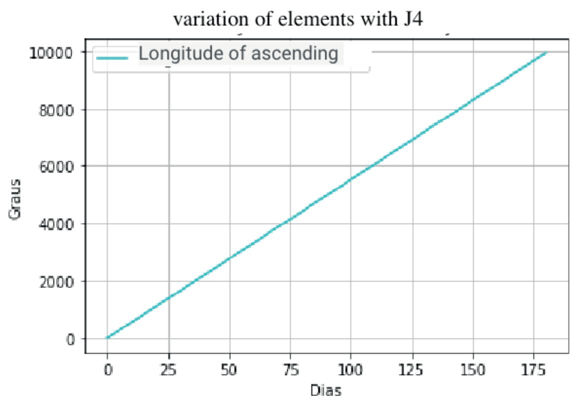

Figure 2.28 - Longitude at the Ascending Node with J4 for parameters 2.

Source: Author's production.

CONCLUSION

It is verified through this study that the influences on the disturbances considering the zonal harmonics become noticeably large from J3 onwards, with J4 being the harmonic that most influenced the orbits, mainly in relation to the degrees of inclination and the eccentricity of the orbit. Such results produced are only for the separate harmonics, and lead us to believe that J5, J6 and C22 result in even greater influences on satellites orbiting the Moon, and such hypotheses can be studied with subsequent studies.

Furthermore, in addition to studying the influence of harmonics separately, for a more complete and clear result on all the disturbances studied in the orbits, the sum of the harmonics must be taken into consideration, when calculating the graphs in order to obtain greater understanding regarding the influence that the harmonics together perform on the orbit in question.

THANKS

To the National Council for Scientific and Technological Development (CNPq) for the scholarship through the Institutional Program for Scientific Initiation Scholarships (PIBIC/INPE) and Proc 316006/2023-8.

REFERENCES

BEUTLER, G., MERVART, L., VERDUN, A**. Methods of Celestial Mechanics: Theory, Applications and Computer Programs**, Vol. 1, Springer, Berlin, 2005.

BROUWER, D. and CLEMENCE, G. **Methods of Celestial Mechanics**. 3ª ed. New York: Academic Press, 1961.

CARVALHO, J. P. S.; PRADO, A. F. B. A.; Vilhena de Moraes, R. . **Some orbital characteristics of lunar artificial satellites**. Celestial Mechanics & Dynamical Astronomy, v. 108, p. 371-388, 2010.

CARVALHO, J. P. S.; PRADO, A. F. B. A.; Vilhena de Moraes, R. . **Planetary Satellite Orbiters: Applications for the Moon**. Mathematical Problems in Engineering, doi :10.1155/2011/187478, 2011.

CARVALHO, J. P. S., VILHENA DE MORAES, R., PRADO, A. F. B. A.

Nonsphericity of the Moon and Near Sun-Synchronous Polar Lunar Orbits. Mathematical Problems in Engineering, doi: 10.1155/2009/740460, 2009.

CHOBOTOV, V.A. **Orbital Mechanics**. 3 a. ed Virginia: AIAA Educational Series, 2002.

KUGA, H. K., RAO, K. R., CARRARA, V. **Introdução** à **Mecânica Orbital**, 2ª Edição, INPE, S. J. Campos - SP, 2008.

KUGA, H. K., RAO, K. R., CARRARA, V. **Satélites Artificiais, Movimento Orbital**, 1ª Edição, INPE, S. J. Campos - SP, 2011.

MORANDO, M. B. **Mouvement d'un satellite artificiel de la Terre**. Gordon & Breach, Paris, 1974.

PRADO, A. F. B. A. and KUGA, H. H. **Fundamentos de Tecnologia Espacial**. São José dos Campos: INPE, 2001.

VILHENA DE MORAES, R. **Trajetória de Veículos Espaciais**, São José dos Campos, Publicação Interna, ITA, 1978.

WALTER, U. **Astronautics: The Physics of Space Flight**, Wiley/VCH, Weinmach, 2008.

WILLIAMS, David R. Soviet Lunar Missions. **NASA Space Science Data Coordinated Archive**, 2005. Disponível em: https://nssdc.gsfc.nasa.gov/planetary/lunar/lunarussr.html#:~:text=The%20Soviet%20L unar%20program%20had,probe%20to%20return%20to%20Earth. Acesso em 28 de set. de 2022.

CHANG'E 5 Test Mission. **Spaceflight 101**, 2022. Disponível em: https://spaceflight101.com/change/change-5-test-mission/. Acesso em 28 de set. de 2022.